

## Article

# Verification of the Influence of Particle Shape on the Chemical Resistance of Epoxy Coating and Use of Waste Glass as the Filler

Jana Hodná<sup>1</sup>, Jakub Hodul<sup>1,\*</sup> , Rostislav Drochytka<sup>1</sup>  and Michaela Seidlová<sup>2</sup>

<sup>1</sup> Faculty of Civil Engineering, Brno University of Technology, 602 00 Brno, Czech Republic; hodna.j@fce.vutbr.cz (J.H.); drochytka.r@fce.vutbr.cz (R.D.)

<sup>2</sup> IN-CHEMIE Technology s.r.o., 779 00 Olomouc, Czech Republic; michaela.seidlova@in-chemie.cz

\* Correspondence: hodul.j@fce.vutbr.cz; Tel.: +420-541-147-530

**Abstract:** The use of suitable secondary raw materials as fillers in progressive, protective agents primarily intended for horizontal concrete construction is very effective not only from the ecological but also from the economic point of view. The impact of using various types of waste glass as fillers on the mechanical parameters of epoxy coatings was experimentally verified. Assessing the dependency of the coating's chemical resistance on the shape of the used filler's particles was the main aim of the performed research. A solvent-free epoxy suitable for a chemically aggressive environment was selected for the experiment. These were epoxy coatings filled with a micro filler based on raw materials such as glass flakes and silica flour. Three tested formulations containing fillers with different particle shapes and characteristics were exposed to H<sub>2</sub>SO<sub>4</sub>, HCl, CH<sub>2</sub>O<sub>2</sub> and NaOH at concentrations of 5% and 30% and evaluated after 60, 90 and 120 days. The chemical resistance assessment was carried out not only visually but also using a scanning electron microscope (SEM). Thanks to the use of the waste glass as a coating filler, tensile properties and hardness improved, and its use did not negatively affect the chemical resistance and adhesion of the epoxy coatings. It was found that the shape of the filler particles influences the resistance of the coating against a chemically aggressive environment. The epoxy coating containing pre-treated waste windshield glass (shards) showed even better properties than the reference coating.

**Keywords:** epoxy resin; coating; microstructure; chemical stress; glass flakes; silica flour; waste glass; particle shape



**Citation:** Hodná, J.; Hodul, J.; Drochytka, R.; Seidlová, M. Verification of the Influence of Particle Shape on the Chemical Resistance of Epoxy Coating and Use of Waste Glass as the Filler. *Coatings* **2022**, *12*, 309. <https://doi.org/10.3390/coatings12030309>

Academic Editor: Alina Vladescu

Received: 26 January 2022

Accepted: 21 February 2022

Published: 24 February 2022

**Publisher's Note:** MDPI stays neutral with regard to jurisdictional claims in published maps and institutional affiliations.



**Copyright:** © 2022 by the authors. Licensee MDPI, Basel, Switzerland. This article is an open access article distributed under the terms and conditions of the Creative Commons Attribution (CC BY) license (<https://creativecommons.org/licenses/by/4.0/>).

## 1. Introduction

Currently, the most used agents for protecting metal or silicate horizontal constructions against corrosion caused by various influences are polymer-based materials [1–3]. They are used during construction as preventive protection as well as reconstruction and repairs as repair and sanitation mortars, fulfilling not only a protective but also an esthetical and technical function, e.g., as industrial flooring [4]. Polymer materials show high strength and exceptional durability, quickly harden and can use waste glass as a filler [5–7]. A polymer binder based on epoxy resin, which is known for its excellent strength, surface hardness, bond to cement-based composites and resistance against aggressive substances, was selected for this research [8]. The formulation of the epoxy coating affects the chemistry of polymer chain formation and the molecular weight. The ultimate form of the polymer chain and its length, shape and configuration determine the properties and physical characteristics of the coating, such as its flexibility, hardness and adhesion [9,10].

The issue of waste production in everyday life, construction and other industrial fields is currently a major issue [11–13]. Waste and its subsequent disposal are global problems currently solved by modifying waste legislation but also by finding innovative ways to repurpose it. One possibility is using waste in newly developed building materials [14–16].

Within the research and development of progressive, protective agents for horizontal construction, we focused on finding a new utilisation of secondary materials that would otherwise be disposed of. Specifically, the possibility of repurposing recycled glass from different sources as a filler in polymer coatings was examined [17]. Various studies state that by adding different types of fillers and nanofillers, it is possible to improve the physico-chemical properties of polymers [18]. These fillers can also improve the barrier protection of polymer coatings and reduce the permeability of aggressive substances into coatings [19,20]. The properties of polymer nanocomposites may affect their inner properties, chemical functional groups, morphology, size and amount [21,22].

Glass flakes (GF) and silica flour, produced by grinding selected pure silica sands, are commonly used fillers ensuring a better resistance of a protective material against chemicals. GF, as two-dimensional materials with flat and smooth surfaces, have a high side ratio. They show chemical inertia, low permeability to water steam and high abrasion resistance [23]. The incorporation of nano-GF into polymer coatings improves the properties of an organic matrix, such as lower reduction and shrinkage, increasing size stability, surface hardness, wear-and-tear resistance, tensile and flexural strength and high resistance against weathering and chemical influences [24,25]. Polymers filled with flake pigments are widely used in the chemical industry for protection against corrosion of silicates and metal surfaces, mainly due to their positive influence on reducing the rate of penetration of aggressive substances into the protective coatings [26].

An alternative to conventional fillers is the use of secondary raw materials. Glass is a potential alternative for filling polymer materials due to its high content of  $\text{SiO}_2$ . Additionally, waste glass is produced in several industrial fields, and if it is not reused in production, it becomes waste that needs to be dumped: for instance, glass waste from car windshields, glass bottles, solar collector glass tubes, chemical glass production or foam glass. However, these wastes must be modified in several ways such as removing foil and impurities, washing, drying, crushing, grinding and sorting, in order to obtain the required fraction.

The research and development of progressive protective materials for horizontal structures with the use of secondary raw materials, namely, the design and verification of the incorporation of waste substances into new polymer coatings, is a very important topic at present. The introduction of such types of coatings into standard production would be entirely innovative, but it is only necessary to select suitable secondary raw materials that meet the requirements for coating fillers and to verify the properties of the resulting materials. Suitable waste glass replaces commonly used fillers, thus ensuring a reduction in the price of polymer coatings, and maintaining or improving the physical–mechanical parameters and chemical resistance of coatings. New polymer coatings containing secondary raw materials can serve as protective materials against corrosion of concrete horizontal structures—mainly as industrial floors and protective coatings that will protect structures not only from external climatic influences, but also against aggressive chemical environments—and thus ensure their longer service life. It is possible to use all developed and verified materials as well as repair materials for concrete structures. The advantage of these materials is their more environmentally friendly composition, but also their lower purchase price. These materials also offer new possibilities for filling coatings, and they also allow the possible consumption of waste materials and thus ensure environmental protection. The shape of particles of waste glass and other used micro fillers can have an impact not only on the mechanical parameters but also on the chemical resistance of coatings. The aim of this study was to experimentally verify formulations of polymer coatings with an optimal content of secondary raw materials as micro fillers that meet the properties required for their use in an aggressive environment, and to verify the used filler particles' influence on the resulting chemical resistance of the protective coating. Using these waste raw materials will save irreplaceable natural resources—such as silica sand—and limit their extraction from negatively affecting the environment.

## 2. Materials

### 2.1. Polymer Binder

Solvent-free epoxy resin was used as a binding basis. It is a pigmented, low-viscosity, two-component material with high chemical resistance. The resulting surface composed of this material shows resistance against acids, alcohols and oil substances, which is why it is intended for use as anticorrosive and anti-chemical protection of metal constructions—tanks—and for inner insulation protection of concrete sediment tanks, wastewater treatment plants and sumps. This material can also be used as a floor coating. The mixing ratio of the A component, epoxy resin, to the B component, hardener, on a polyamine base was 2:1. The processability of the mixed material at 20 °C was 40 min.

### 2.2. Fillers

In a polymer matrix, a filler not only ensures its subsequent strength and hardness [27] but also increases its so-called barrier performance [28] and reduces the material price. Since commonly used materials for filling epoxy materials have a high SiO<sub>2</sub> content, waste glass seems to be an ideal alternative. Waste glass and silica sand were ground in a ball mill for 45 min and then processed through a sieve of 0.063 mm. The particle size distribution for both the reference and waste fillers is presented in Figure 1, their chemical composition is presented in Table 1 and their specific gravity is presented in Table 2. Determination of the chemical composition of the fillers was performed in an accredited test laboratory at LABTECH Ltd. Individual determinations were performed according to the standards EN ISO 11885, ČSN 72 0105-1, ČSN 720,103 and ČSN 720100.

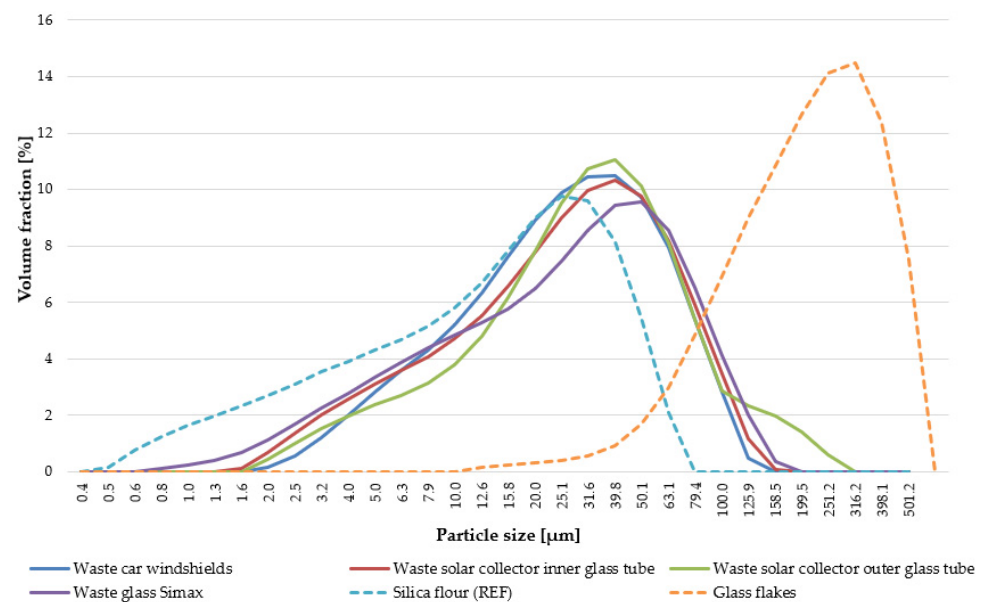


**Figure 1.** Particle size distribution for both the reference and waste fillers.

#### 2.2.1. Glass Flakes (GF)

Glass flakes (GF) are industrially produced, very thin, flat plates with smooth surfaces that are transparent and have a neutral colour. Protective coatings using this filler are used in various industrial fields, especially where it is necessary to ensure better protection against aggressive substances: for example, the chemical industry, the petrochemical industry, the food industry and in health care, and they have been used since 1970 [29]. As a reinforcement, they improve resistance against chemicals and increase strength [30]. In terms of colour, they can also be used as pigments with a unique effect.

**Table 1.** Chemical composition of the fillers (% dry matter).

Parameter	GF	REF	CW	STi	STo	SIM
LOI <sup>1</sup>	0.32	0.29	0.65	0.30	0.33	0.31
SiO <sub>2</sub>	74.6	99.3	71.8	70.9	71.2	79.4
Al <sub>2</sub> O <sub>3</sub>	4.51	0.174	1.05	3.93	3.95	2.28
Fe <sub>2</sub> O <sub>3</sub>	0.191	0.026	0.17	0.045	0.049	0.015
TiO <sub>2</sub>	0.021	0.021	0.03	0.018	0.014	0.011
MnO	0.006	0.001	<0.001	0.001	0.001	<0.001
CaO	6.91	0.028	9.39	5.12	5.01	0.68
MgO	2.29	0.008	3.91	2.59	2.54	0.59
K <sub>2</sub> O	2.52	0.102	0.52	2.87	2.97	1.8
Na <sub>2</sub> O	8.92	0.029	12.0	12.17	11.89	1.9
Li <sub>2</sub> O	0.002	<0.001	0.004	<0.001	<0.001	<0.001
Cr <sub>2</sub> O <sub>3</sub>	<0.004	<0.004	0.005	0.004	0.004	<0.004
BaO	0.007	0.011	0.17	1.99	1.99	0.004
ZrO <sub>2</sub>	0.021	0.008	0.29	0.028	0.019	0.009
B <sub>2</sub> O <sub>3</sub>	<0.005	<0.005	<0.005	<0.005	<0.005	13.0
PbO	<0.001	<0.001	0.011	<0.001	<0.001	<0.001
SrO	<0.004	<0.004	<0.004	0.0252	0.0325	<0.004

<sup>1</sup> Loss on ignition.

**Table 2.** Specific gravity of the fillers in kg/m<sup>3</sup>.

GF	REF	CW	STi	STo	SIM
2470	2660	2540	2500	2520	2290

GF are characterised depending on their thickness, size and original glass composition. Flake thickness can be measured either manually by a scanning electron microscope or automatically using innovative spectroscopy techniques. The Glassflake Ltd. company (Leeds, UK) produces flakes of 7 to 100 µm. The principle of using GF in polymer coating materials is as follows: Thanks to the flakes' morphology, meaning the ratio of the high side against the surface of a flake, and their precise planar layout, mutually to each other and the base, they create a slatted barrier in the material. If the surface of the material is in contact with an aggressive substance, this barrier creates a winding path and increases the track length that the aggressive media must overcome through the coating. This ensures a longer surface durability over time compared to non-filled coatings or coatings filled by a grain or fibre filler [31].

### 2.2.2. Silica Flour (REF)

Silica flour is obtained from dried silica sands in graded grain sizes. In systems with artificial resins, mixtures can reach a higher density compared to individual fractions. As a result, they reduce the consumption of resin and increase the strength of the resulting products. The shape of silica flour particles is irregular, with most edges being rounded.

### 2.2.3. Waste Car Windshields (CW)

At present, many types of car windshields accommodate acoustic, atmospheric, thermal and visual comfort as well as safety and protection. The composition of windshields is very different compared to classic glass because some contain resins, tinting plating and protection films. A standard sorting line for package glass cannot sort or adjust car windshields. Classic glassworks also do not have the needed equipment for processing car windshields, which is why these are usually stored. Car windshields can be divided into two types according to their use: windshields containing a protection film, and windshields without a film.

As part of the pre-treatment in our research, the protection film was removed first. If the windshield glass was broken, the film was cut with a box cutter and then ground in a

ball mill where the glass was separated from the polymer film contained in the windshields. The total weight of the material for grinding was 3 kg of glass shards. Furthermore, the ground glass was manually sieved to a fraction of  $\leq 0.063$  mm.

#### 2.2.4. Waste Solar Collector Glass Tube (ST)

Solar collector glass tubes were the first type of solar panel and consist of two cylinders embedded in each other (Figure 2). The inner cylinder—the dark glass—surrounds the copper indium gallium diselenide (CIGS) solar cell, which is protected by the outer cylinder and a special silica fluid in the interspace. The outer cylinder (the bright glass—STo) refracts the incident light and leads it directly to the cell regardless of the angle at which the light rays strike the cell. In this way, solar energy is maximumly used—from one cell to the entire roof.

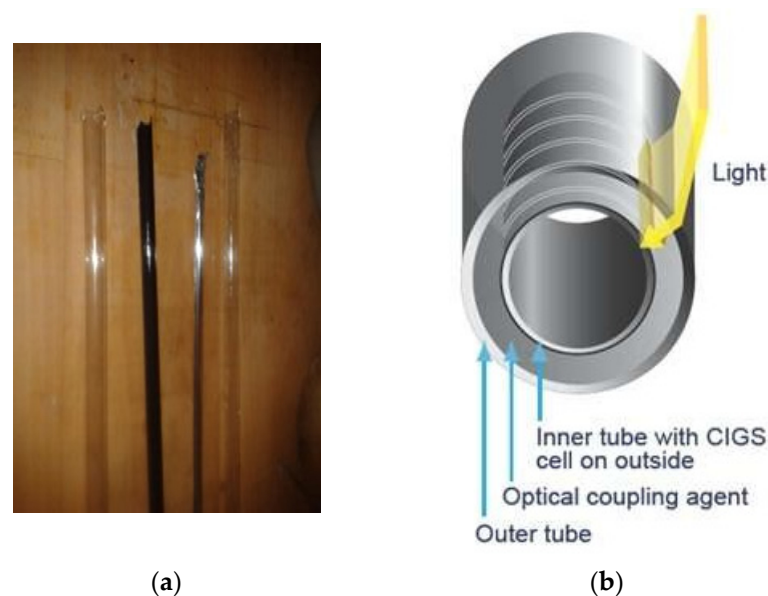


**Figure 2.** Solar collector glass tube (ST): (a) waste solar collector glass tube used after grinding as the filler in the coating; (b) section of a tubular solar panel [32].

The tube panel used was supplied by the iSolar, s.r.o. company (Pardubice, Czech Republic) as a disposed of and broken piece. The panel was disassembled by removing the metal frame and breaking down individual tubes into parts according to the material type—the inner, dark glass, the plastic tube, aluminium foil, silica fluid and the outer, light glass. The inner, dark glass (Sti), which is in contact with the silica fluid, and therefore very greasy, had to be washed in a degreasing agent and then dried in a drying room. Then, the material was ground and sorted to the required fraction, whereby two types of filler were produced: dark filler from the inner glass and light filler from the outer glass. Particles from both glass types were sharp-edged without rounded parts.

#### 2.2.5. Waste Glass SIMAX (SIM)

Thanks to its chemical composition and properties, SIMAX glass belongs to the group of transparent, hard borosilicate glasses, which have exceptional thermal and chemical resistance. SIMAX offers a wide spectrum of products for technical and laboratory glass, industrial equipment or kitchen glassware. Products made of SIMAX glass are smooth and non-porous, perfectly transparent and corrosion-resistant, even in demanding service environments up to 300 °C without a sudden temperature change. SIMAX glass is eco-friendly and, from an ecological point of view, absolutely harmless.

Due to its properties, SIMAX glass is used where the highest requirements are placed on products in terms of thermal and chemical resistance and neutrality against substances or preparations that are in contact with them, i.e., in chemistry, petrochemistry, the food

industry, energetics, metallurgy, health care, microbiology, the pharmaceutical industry, mechanical engineering and laboratories. The glass is etched only by hydrofluoric acid and concentrated trihydrogen phosphoric acid, and concentrated hot alkali solutions corrode the glass. The corrosion is also increased by continually altering the acidic and alkaline environment. During production in the Kavalierglass, a.s. (Sázava, Czech Republic) machines, undesirable waste in the form of pressing waste cannot be reused. SIMAX particles have the shape of sharp shards.

### 2.3. Tested Coating Formulations

The amount of filler was the same for all formulations, namely, 25 wt.% of the binder amount. This filler value was chosen due to its optimum workability, applicability and viscosity and the resulting surface of the coating materials. A material filled with 25 wt.% of silica flour (NBR-REF) was used as a reference coating for comparing the mechanical properties of the tested coatings. The formulations of the coating materials, which underwent testing of mechanical parameters, are presented in Table 3. To compare the particle shape's influence on the chemical resistance of the coatings, formulations NBR-GF, NBR-REF and NBR-CW were selected.

**Table 3.** Formulations of the epoxy coatings for testing of basic parameters.

Type of Coating	Epoxy Resin (wt.%)	Hardener (wt.%)	Filler (wt.% of Binder)	Type of Filler
NBR-GF	75	25	25	Glass flakes (GF)
NBR-REF	75	25	25	Silica flour (REF)
NBR-CW	75	25	25	Waste car windshields (CW)
NBR-STi	75	25	25	Waste solar collector glass tube—inner (STi)
NBR-STo	75	25	25	Waste solar collector glass tube—outer (STo)
NBR-SIM	75	25	25	Waste glass SIMAX (SIM)

## 3. Methods

### 3.1. Adhesion on Concrete Substrates

The test was performed according to the standard EN ISO 4624—Paints and varnishes—Pull-off test for adhesion [33]. During testing, the force needed for removing the coating from the concrete base was measured. The result of the test was the tensile stress needed for damaging the weakest interface, i.e., adhesive damage, or the weakest part, i.e., cohesion damage, of the tested set. There can also be both types of failure.

Various bases can be used for the test. Because the tested coatings are mainly intended for concrete coatings, a concrete pavement made of C16/20 class concrete was used for the test. The coating was applied on the concrete base by a metal trowel in two layers; each layer had a thickness of around 250 µm. Testing of adhesion to concrete was carried out after 28 days from the application of the coating on the base; the pull-off adhesion tester Elcometer 506-20D (Elcometer Ltd., Manchester, UK) was used for this purpose.

### 3.2. Shore D Hardness

The hardness of polymer coatings containing secondary and primary raw materials was tested according to the standard EN ISO 868—Plastics and ebonite—Determination of indentation hardness by means of a durometer (Shore hardness), [34]. The indentation hardness by indenting a specified tip into the material under specified conditions was examined during this test. The hardness value is inversely proportional to the depth of the indenting tip and depends on the elastic modulus and the viscoelasticity properties of the material. The Shore durometer LD0551—the D-type tip (TQC Sheen, Molenbaan, The Netherlands) was used for this test.

### 3.3. Tensile Properties

A tensile test is performed to explore the relationship between the microstructure and tensile properties and determine whether an epoxy material could fulfil the mechanical property requirements for application in a chemically aggressive environment, e.g., concrete sewers and the chemical industry [35]. The test of tensile properties was carried out to better evaluate an eventual crack bridging. Tensile properties of the epoxy coatings were determined according to the EN ISO 527-1 and EN ISO 527-2 standards [36,37]. Based on these standards, the specimens—dog bones of the 1B type—were tested for the relative elongation and the tensile stress at the first break. During the testing, an extensometer with an original length of  $L_0 = 50$  was used. Specimens were extended in the direction of their axis at a constant testing rate of 5 mm/min until they broke. Three specimens from each formulation were tested 28 days after their laboratory preparation in silicon triple moulds.

### 3.4. Influence of Particle Shape of Filler on Chemical Resistance

This test was not normative; its methodology was designed to be feasible under laboratory conditions and to be evaluable. During this assessment, the particle shape's influence on the chemical resistance of the material, which was the NBR epoxy coating with various fillers, was tested.

The selected formulations were the best from the basic testing, and the fillers used differed most in particle shape and were first applied on concrete pavements. After 28 days, they were exposed to 5% and 30% solutions of  $H_2SO_4$ , HCl,  $CH_2O_2$  and NaOH. Specimens were stored in an environment with a temperature of  $23 \pm 2$  °C and humidity of  $50 \pm 5\%$ ; they were evaluated after 60, 90 and 120 days.

When concentrated, sulphuric acid is a dense, oily fluid infinitely miscible with water. It is a very dangerous corrosive and causes the dehydration of organic substances. However, diluted sulphuric acid does not have abilities and reacts with non-noble metals under the formation of hydroxide and sulphates.  $H_2SO_4$  is produced in sewage systems within biocorrosion and by the action of sulphuric bacteria and is then used in treating swimming pool water or as an electrolyte for filling dry maintenance lead-acid batteries. HCl is another strong corrosive acid that can be used industrially to process steel used in the building and construction industry.  $CH_2O_2$  is an ingredient in ant poison and is mainly used in organic technology. Formic acid is used for dye production, rubber production and tannery for descaling the leather. NaOH is used for soap production, in the textile industry and for treating drinking water. The stated chemically aggressive environments were selected for executing the research of possible operations and environments in which the materials will be used.

#### 3.4.1. Visual Assessment

During the exposure of polymers to chemicals, their degradation may occur due to the adverse chemical reaction of the polymers with their surroundings. The breakage of chemical bonds of the polymer chain and its degradation occur upon this reaction. Many possible chemical reactions result in polymer damage. Thus, depolymerisation occurs during the degradation process [38].

The polymer coating can manifest a change in its properties, which causes visible damage to the surface, such as cracking, bobbing, colour changes and other types of degradation. At a higher level of exposure of polymers to chemicals, chemical degradation of the polymer may occur; therefore, the breakage of cross-linking chains occurs. All changes in properties are influenced by the type, temperature and concentration of a chemical as well as the exposure time [39]. An evaluation system [40], as shown in Table 4, was applied for the visual assessment of the changes in epoxy coatings.

#### 3.4.2. Microscopic Analysis

The microstructure of the epoxy coatings loaded in a chemically aggressive environment was monitored using a scanning electron microscope (SEM), MIRA3 XMU type

(TESCAN, Brno, Czech Republic,)); the most suitable magnification for monitoring was 500×. Not only the principle of the coating's degradation but also the size, type and distribution of the filler particles in the epoxy binder were monitored.

**Table 4.** Evaluation system for assessing chemical resistance from a visual point of view.

Evaluation <sup>1</sup>	Description of the Observed Change on Coating
1	without any changes
2	only colour changes
3	detachment from the substrate, without further damage
4	detachment from the substrate and cracking
5	complete damage

<sup>1</sup> Minimum change = 1; maximum degradation = 5

## 4. Results and Discussion

### 4.1. Mechanical Parameters

#### 4.1.1. Adhesion on Concrete

The need for adhesion monitoring exists in the case of large areas of chemically stressed objects such as industrial floors, bridge decks and injected concrete structures [41]. Based on the evaluation of coating adhesion on concrete substrates using a pull-off adhesion gauge (Table 5), it can be seen that the adhesion of coatings to concrete was higher than the tensile strength of the concrete. The coatings showed a minimum adhesion to the concrete of 2.5 MPa. The average value of adhesion was determined from three measurements, and the place of failure was always the same. Substrate—concrete—failure was achieved with all samples.

It has been claimed that inadequate coating adhesion, along with the presence of discontinuities in the coating, may lead to film undercutting and early breakage of the coating from the concrete substrate protection system [42].

**Table 5.** Evaluation of the coating adhesion on concrete substrates.

Coating	Adhesion (MPa)	Failure Mode
NBR-GF	4.7	Substrate failure
NBR-REF	4.9	Substrate failure
NBR-CW	2.5	Substrate failure
NBR-STi	3.1	Substrate failure
NBR-STo	3.2	Substrate failure
NBR-SIM	3.3	Substrate failure

#### 4.1.2. Shore D Hardness

A graphical evaluation of the Shore D hardness is illustrated in Figure 3. The surface hardness of the tested coatings did not differ very much, while the highest value was 89 for the NBR-CW coatings containing waste windshield glass—shards—as a filler. The surface Shore D hardness value depends primarily on the type of polymer resin used [43], while epoxy coatings showed higher hardness than polyurethane coatings. The type of waste glass used also did not significantly affect the hardness of the epoxy coatings.

The hardness of polymeric coatings also has statistically significant effects on the coating abrasive wear resistance [44]. The hardness and elastic modulus showed a maximum value close to the surface, followed by a plateau and a significant increase at higher penetrations [45].

#### 4.1.3. Tensile Properties

Figures 4 and 5 show a graphical evaluation of the tensile properties—tensile stress and tensile strain at the first break. The tensile strength was around 40 MPa for all tested formulations. The highest value was obtained for the NBR-CW coating, which also showed

the highest surface hardness. As regards the above stated mechanical parameters, the resin used is also important to the tensile properties. Epoxy coatings generally show low relative elongation due to their higher elasticity modulus. The crack in the concrete substrate does not move any further if the stress is lowered to values smaller than the minimum necessary for crack propagation. If a viscoelastic membrane with high tensile stress and proper tensile strain is applied, it can withstand the crack movement in the substrate [46].

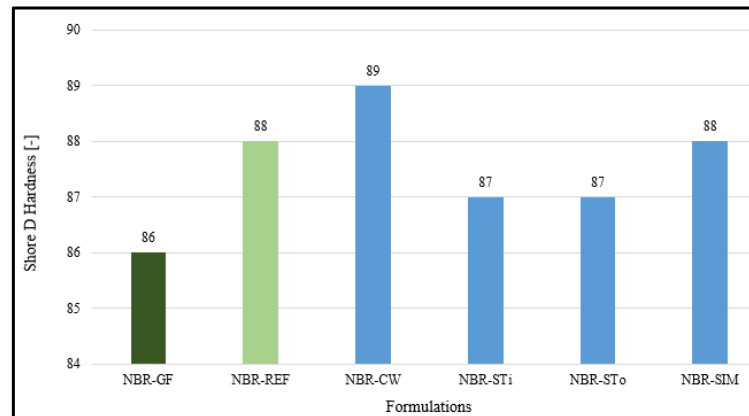


Figure 3. Shore D hardness of the epoxy coatings with different fillers.

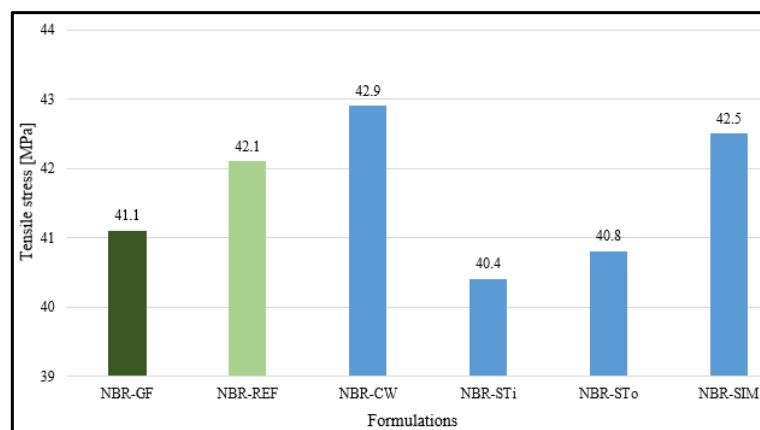


Figure 4. Tensile stress at first break of the epoxy coatings with different fillers.

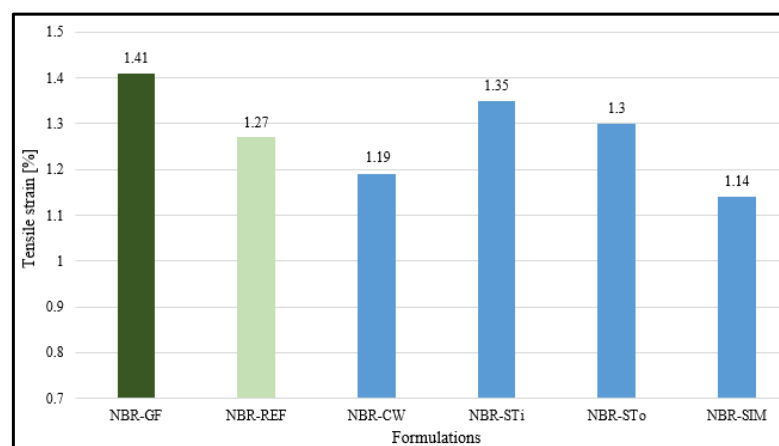


Figure 5. Tensile strain at first break of the epoxy coatings with different fillers.

Zheng et al. [47] reported that adding 3% SiO<sub>2</sub> into the epoxy matrix increases the tensile strength and impact strength by 115% and 56%, respectively. The improvement in

the mechanical properties of the epoxy coatings depends on the adhesion of the filler to the epoxy matrix and the dispersion of the filler in the epoxy matrix [48].

#### 4.2. Influence of Particle Shape of Filler on Chemical Resistance

Based on the basic tests' results stated in Section 4.1, it can be concluded that the monitored properties of the NBR coating using 25% of waste windshield glass—shards—were very similar to the properties of the reference material, i.e., filler of rounded particles. It was chosen for further testing, namely, testing the filler particle shape's influence on the chemical resistance, which was the focus of this research, not only for this reason but also regarding the specific shape of the particles of ground shards—sharp-edged particles. Furthermore, the NBR-GF formulation containing glass flakes, which were added to the polymer coatings to improve their chemical resistance, and the NBR-REF reference coating were also subjected to this testing. Thus, differently shaped particles were chosen to monitor the influence of the selected filler on the chemical resistance. The contact zone between the filler and the binder was also unique for all tested formulations. This test was not normative; its methodology was designed to be applicable under laboratory conditions and to be evaluable.

##### 4.2.1. Visual Assessment

The visual assessment evaluation of the chemical resistance of the NBR epoxy coating material containing the silica flour filler with rounded parts—the NBR-REF formulation—is presented in Table 6. It follows from the results that the coating was least resistant against 30% CH<sub>2</sub>O<sub>2</sub>, where complete degradation of the material already occurred after 90 days (5). Generally, the coating was best able to withstand the NaOH solution. Almusallam et al. [49] stated that their epoxy and polyurethane coatings were found to be relatively intact, with just the corners of the specimens damaged, after 60 days in a 2.5% sulfuric acid solution. Dębska et al. [50] found that in their samples of epoxy mortars immersed in aqueous solutions of acids, over time, the connection between the polymer matrix and aggregate weakened, which resulted in an increase in their weight and increasing fragility.

**Table 6.** Evaluation of the visual assessment of the chemical resistance of the NBR-REF coating.

Exposure Time	H <sub>2</sub> SO <sub>4</sub>		HCl		CH <sub>2</sub> O <sub>2</sub>		NaOH	
	5%	30%	5%	30%	5%	30%	5%	30%
60 days	1	1	1	2	1	4	1	1
90 days	1	2	2	2	2	5	1	1
120 days	2	2	2	2	2	5	1	2

In Figure 6a, the colour change of the coating can be seen after exposure to 30% HCl for 90 days, where only the surface colour has changed without any disruption, cracking, etc. Contrastingly, Figure 6b depicts the same coating after 60 days of exposure to the 30% CH<sub>2</sub>O<sub>2</sub> solution when the material peeled off the base and cracked.

The total collapse of the polymer system of the NBR-REF coating with silica flour exposed to a chemically aggressive environment in the form of 30% CH<sub>2</sub>O<sub>2</sub>, which occurred after 120 days of exposure, is obvious from Figure 7.

In recent years, anticorrosive coatings containing glass flakes are being investigated in relation to metal protection in highly corrosive media because they are expected to greatly prevent the aggressive solution's transport through the polymeric matrix [51]. The evaluation of the chemical resistance in terms of the visual assessment according to the NBR-GF assessment system is presented in Table 7. As for the NBR-REF material, the maximum degradation was recorded after exposure to 30% CH<sub>2</sub>O<sub>2</sub>. Similarly, only slight colour changes occurred after exposure to inorganic acids and the NaOH solution.

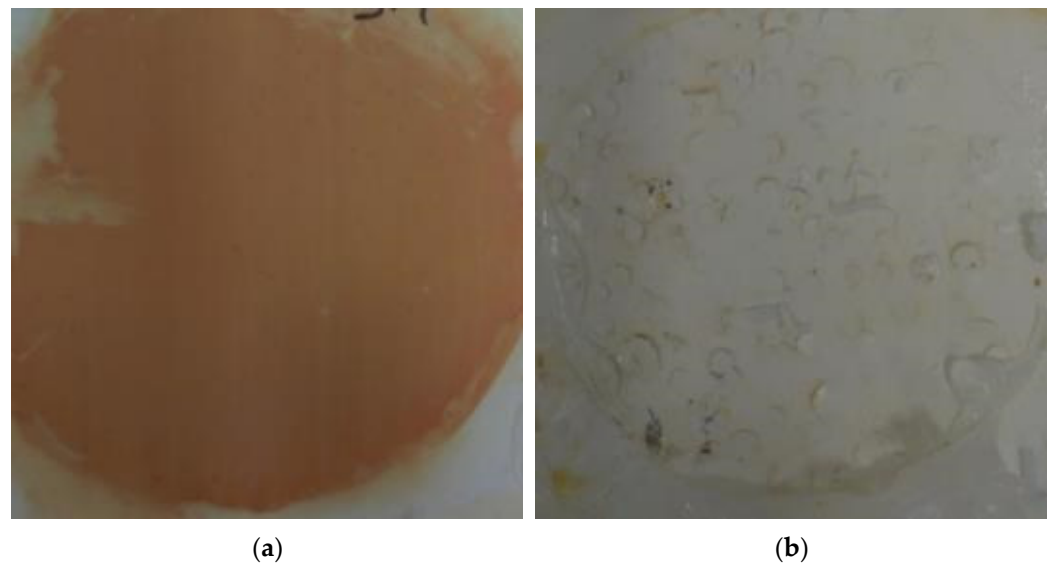


**Figure 6.** NBR-REF coating containing rounded silica particles after chemical loading: (a) colour change of the coating exposed to 30% HCl for 90 days; (b) cracking of the coating exposed to 30% CH<sub>2</sub>O<sub>2</sub> for 60 days.



**Figure 7.** An example of complete degradation of the NBR coating with a filler of rounded particles (NBR-REF) exposed to 30% CH<sub>2</sub>O<sub>2</sub> for 120 days.

**Table 7.** Evaluation of the visual assessment of the chemical resistance of the NBR-GF coating.

Exposure Time	H <sub>2</sub> SO <sub>4</sub>		HCl		CH <sub>2</sub> O <sub>2</sub>		NaOH	
	5%	30%	5%	30%	5%	30%	5%	30%
60 days	1	1	1	1	1	4	1	1
90 days	1	2	1	2	2	5	1	2
120 days	2	2	2	2	2	5	1	2

Figure 8a shows the surface of the NBR-GF coating sample exposed to 30% H<sub>2</sub>SO<sub>4</sub> for 120 days, where only a colour change occurred. Pacheco-Torgal et al. [52] stated that the use of the polymer impregnation process or coatings enhances the chemical resistance of hardened concrete used in the pipe industry against sulphuric acid. Figure 8b illustrates the degradation of the polymer system after 90 days of exposure to 30% CH<sub>2</sub>O<sub>2</sub>, when glass flakes, in this case, as a filler, ensured the cohesion of larger pieces of the tested surface; therefore, the surface released from the base in cohesive pieces. It follows that the filler

in the glass flakes has a positive influence on the chemical resistance against the tested organic acid.

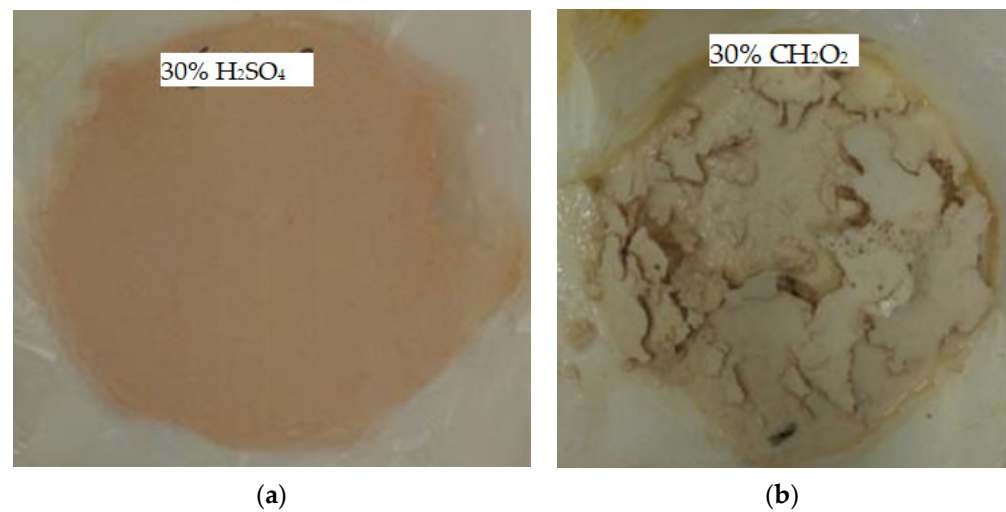


**Figure 8.** Coating NBR-GF after chemical stress: (a) colour change of the coating exposed to 30%  $\text{H}_2\text{SO}_4$  for 120 days; (b) cracking of the coating exposed to 30%  $\text{CH}_2\text{O}_2$  for 90 days.

Figure 9 illustrates the NBR-GF coating containing glass flakes after another 30 days of exposure to 30%  $\text{CH}_2\text{O}_2$ —after 120 days in total—when initially cohesive pieces of the tested material almost degraded to dust, and the use of glass flakes did not prevent this significant degradation.



**Figure 9.** Complete degradation of the NBR-GF coating exposed to 30%  $\text{CH}_2\text{O}_2$  for 120 days.

The evaluation of the chemical resistance of the coating containing sharp-edged shards from waste windshield glass (NBR-CW) as a filler is presented in Table 8. By comparing the evaluation with other coatings containing only primary raw materials, it is possible to notice that the NBR-CW coating containing a secondary raw material shows slightly higher chemical resistance against weakly concentrated solutions. After 120 days of exposure to 5%  $\text{H}_2\text{O}_4$ , there was no colour change on the material's surface. Total degradation of the material after exposure to 30%  $\text{CH}_2\text{O}_2$  occurred anyway; however, after 90 days of exposure to 5%  $\text{CH}_2\text{O}_2$ , no visual changes on the surface of the material were monitored. It is possible to assume that a micro filler in the form of sharp-edged shards slightly improves the chemical resistance of epoxy coatings.

**Table 8.** Evaluation of the visual assessment of the chemical resistance of the NBR-CW coating.

Exposure Time	H <sub>2</sub> SO <sub>4</sub>		HCl		CH <sub>2</sub> O <sub>2</sub>		NaOH	
	5%	30%	5%	30%	5%	30%	5%	30%
60 days	1	1	1	2	1	4	1	1
90 days	1	2	1	2	1	5	1	2
120 days	1	2	2	2	2	5	1	2

Figure 10a shows the surface of the NBR-CW sample in which only a colour change of the material occurred after exposure to 30% HCl for 90 days. After scratching the surface, it was possible to easily remove the coloured layer, by which it was found that the colouring is only superficial and does not go through the whole layer of the surface. Figure 10b captures the colour change and surface cracks of the coating after 120 days of exposure to 5% CH<sub>2</sub>O<sub>2</sub>.

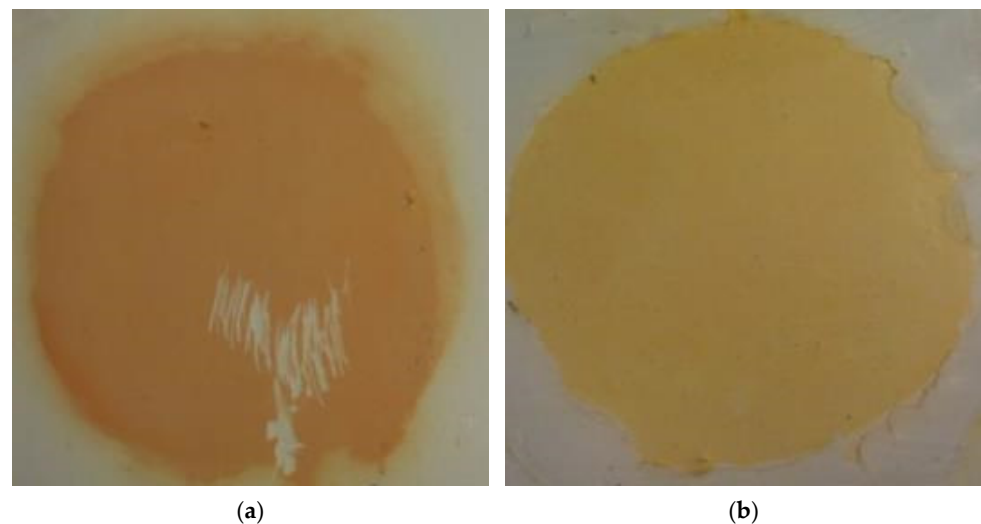


**Figure 10.** The NBR-CW coating: (a) colour change after 90-day exposure to 30% HCl; (b) colour change after exposure to 5% CH<sub>2</sub>O<sub>2</sub> for 120 days.

The visual assessment of the NBR-CW sample filled with ground shards from a windshield after exposure to 30% CH<sub>2</sub>O<sub>2</sub> for 120 days (see Figure 11) was classified by the value of 5—total collapse of the system. This was due to the complete degradation of the tested layer of the coating throughout its thickness.



**Figure 11.** Complete degradation of the NBR-CW coating exposed to 30% CH<sub>2</sub>O<sub>2</sub> for 120 days.

Based on the evaluation of the chemical resistance, it can be concluded that in all tested chemically aggressive solutions, except for 30%  $\text{CH}_2\text{O}_2$ , the degradation of coatings did not start to show visually until 60 days, and therefore it was not necessary to assess the chemical resistance after 30 days of exposure to chemicals. As for 30% formic acid, it can be assumed that the first coating defects occurred after 14 days of exposure to this strong organic acid. Furthermore, it can be assumed that even after 180 days of the coatings' exposure to the selected inorganic acid solutions, the functionality and integrity would not deteriorate significantly. On the other hand, exposure of the epoxy coatings to  $\text{CH}_2\text{O}_2$ , even at a weak 5% concentration, could lead to significant defects in the tested coatings.

The selected concentrations of 5% and 30% proved to be very suitable because it was possible to observe a difference in the resistance of the coatings to solutions of different concentrations, especially for the formic acid. With smaller differences in concentrations, it would not be possible to observe such significant changes in the chemical resistance of the coatings to the selected aggressive solutions. Epoxy coatings are only rarely exposed to higher concentrations of aggressive substances, and therefore solutions with higher concentrations, which could cause greater degradation of coatings, did not need to be tested.

#### 4.2.2. Microscopic Analysis (SEM)

The structure of the NBR polymer coatings exposed to chemical substances was verified by scanning electron microscopy in the samples with a visual assessment of five. For all tested samples, they were always surfaces exposed to formic acid  $\text{CH}_2\text{O}_2$  at a concentration of 30%. Additionally, they were always compared to a material that was not exposed to the chemically aggressive environment but had the same composition—reference coating with rounded particles, reference coating with glass flakes and reference coating with shards. The age of these reference (comparing) coating materials was 120 days. Tasnim et al. [53] stated that SEM analysis showed evidence of micro gaps between fillers and the polymer matrix when exposed to chemicals, and these micro gaps slightly increased in width with an increase in the exposure duration to these solutions.

The SEM picture in Figure 12a shows the structure of the 120-day-old material without exposure to chemicals. The structure has a solid, smooth surface at the fractured edge caused during sampling. It can also be seen that the filler is completely embedded in the polymer, and individual grains are fully coated in the polymer. The material showed no colour changes or disruptions on the surface. It is possible to see several air bubbles in the matrix, which were probably caused by the imperfect mixing of the material prior to its application. Tiny dust particles on the surface were caused by sampling—sample cut-off. Figure 12b illustrates the structure of the same polymer coating after 120 days of exposure to  $\text{CH}_2\text{O}_2$  at a concentration of 30% that is completely disrupted. Rounded grains of a filler protrude from the structure of the composite; they are broken and exposed. The surface degraded to small pieces, which still retain a similar shape and size. The matrix is also degraded, and there is a disruption of the cross-linking chains and depolymerisation of the system. The smaller a molecule of an active chemical, the more aggressive it acts. A smaller molecule can diffuse to the polymer structure more easily and invade the polymer. The chemical resistance of polymers decreases with increasing temperature. Generally, it can be claimed that the better the polymer is cross-linked, the better its chemical resistance [54].

It follows from Figure 13a that after 120 days of storage of the coating in a laboratory environment, the polymer structure is solid and the surface is smooth and has no signs of any disruption, including colour changes. Glass flakes create a stable slatted system; they are not disrupted or exposed in the structure. The polymer matrix is intact, except for tiny air bubbles that were probably caused by the imperfect mixing of the mixture prior to its application. Tiny dust particles on the surface were caused by sampling—sample cut-off. In the micrograph in Figure 13b, it can be seen that the structure of the polymer completely degraded after 120-day exposure to  $\text{CH}_2\text{O}_2$  at a concentration of 30%. Glass flakes protrude from the slatted structure, which is damaged, and grains of the filler are

broken and exposed. The surface is degraded to small pieces, while the grains of the filler are visible even without using a microscope—by the naked eye. The matrix contains air bubbles that were probably caused by the imperfect mixing of the mixture prior to its application.

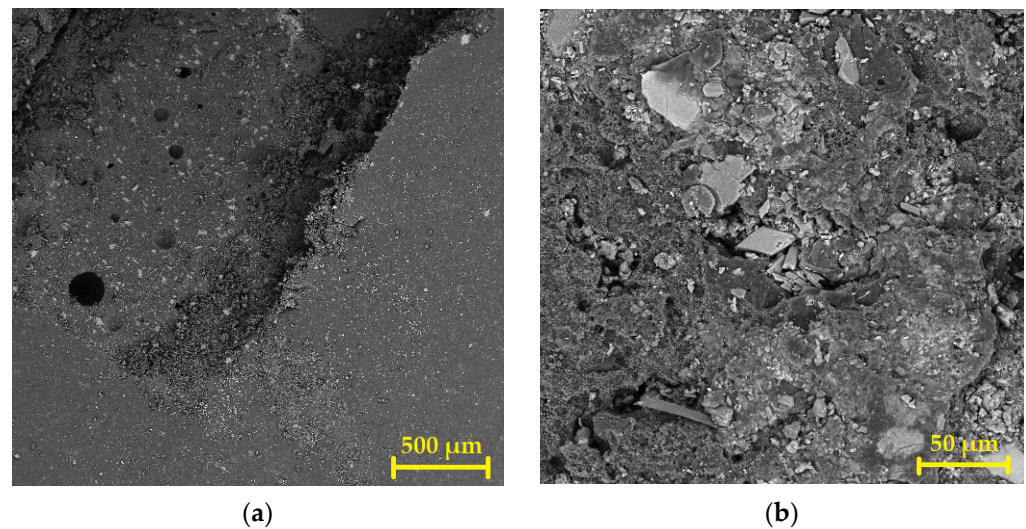


**Figure 12.** SEM photomicrographs of the coating with rounded particles (NBR-REF): (a) reference coating not exposed to the aggressive environment—50× magnification; (b) NBR-REF after exposure to  $\text{CH}_2\text{O}_2$  for 120 days—500× magnification.

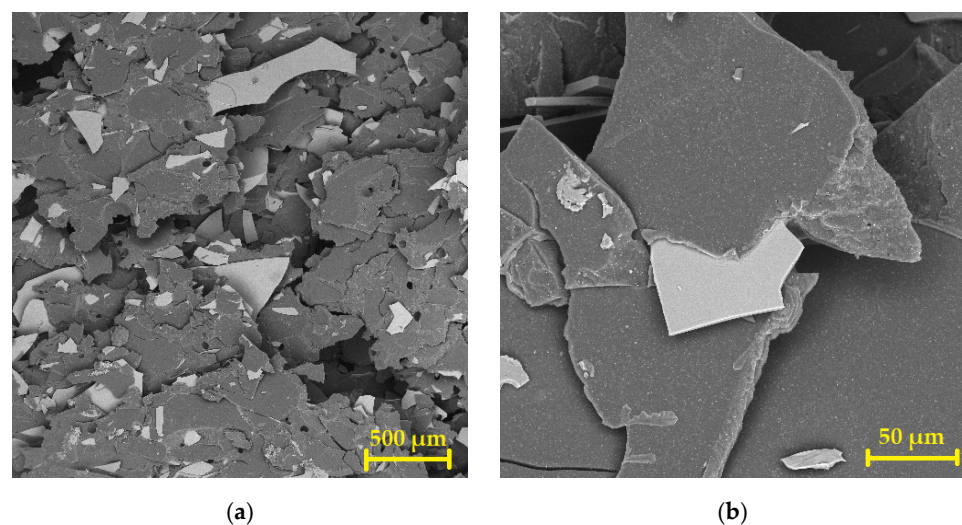


**Figure 13.** SEM photomicrographs of the coating containing glass flakes (NBR-GF): (a) reference coating not exposed to the aggressive environment—50× magnification; (b) NBR-GF after exposure to  $\text{CH}_2\text{O}_2$  for 120 days—500× magnification.

Figure 14a depicts that after 120 days, the structure of the polymer coating NBR-CW stored in laboratory conditions is also solid, and the surface is smooth and has no signs of any disruptions, including colour changes. The grains of the filler are more noticeable on the smooth surface. Particles in the form of shards are completely coated by the polymer matrix, creating a stable, homogeneous structure. Furthermore, it can be observed that individual grains of the filler are evenly distributed in the polymer. The polymer matrix is intact, except for the spots of the sample fracture that were caused during sampling—sample cut-off. In Figure 14b, on the other hand, it is possible to see that the polymer structure is completely disrupted after exposure to  $\text{CH}_2\text{O}_2$  at a concentration of 30% for

120 days. The filler's shards protrude from the disrupted structure, and filler grains are already visible under a microscope at  $50\times$  magnification. The matrix contains air bubbles probably caused by the imperfect mixing of the mixture prior to its application. At a higher magnification, pigment grains that protrude from the polymer matrix are noticeable.

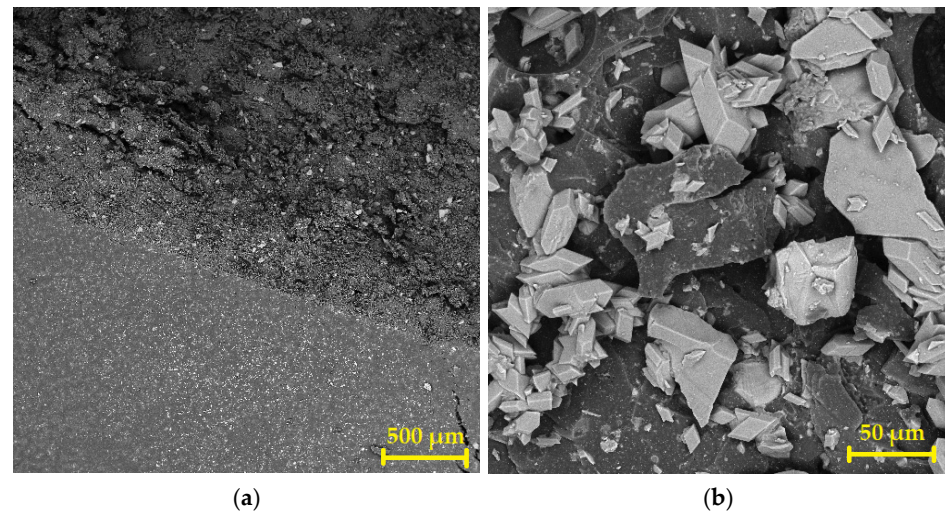


**Figure 14.** SEM photomicrographs of the coating NBR-CW containing shards from a windshield: (a) reference coating not exposed to the aggressive environment— $50\times$  magnification; (b) NBR-CW after exposure to  $\text{CH}_2\text{O}_2$  for 120 days— $500\times$  magnification.

Figure 15a shows waste glass particles (shards) emerging from the polymer matrix, which has been severely disrupted after exposure to formic acid for 120 days. It is possible to observe the sharp edges of shards characteristic of this type of filler. Figure 15b shows the microstructure of the strongly degraded NBR-REF coating, showing that  $\text{CH}_2\text{O}_2$  also disrupted the structure of the quartz flour particles. By comparing these SEM images, it can be concluded that the coating containing shards from a windshield resists the selected chemically aggressive environment better than the reference coating. The incorporation of glass flakes in the polymer matrix can be seen in Figure 16a—the flakes are perfectly coated with an epoxy matrix. Figure 16b shows the disruption of the contact zone between the flakes and the polymer matrix after 90 days of the coating's exposure to 30%  $\text{CH}_2\text{O}_2$ .

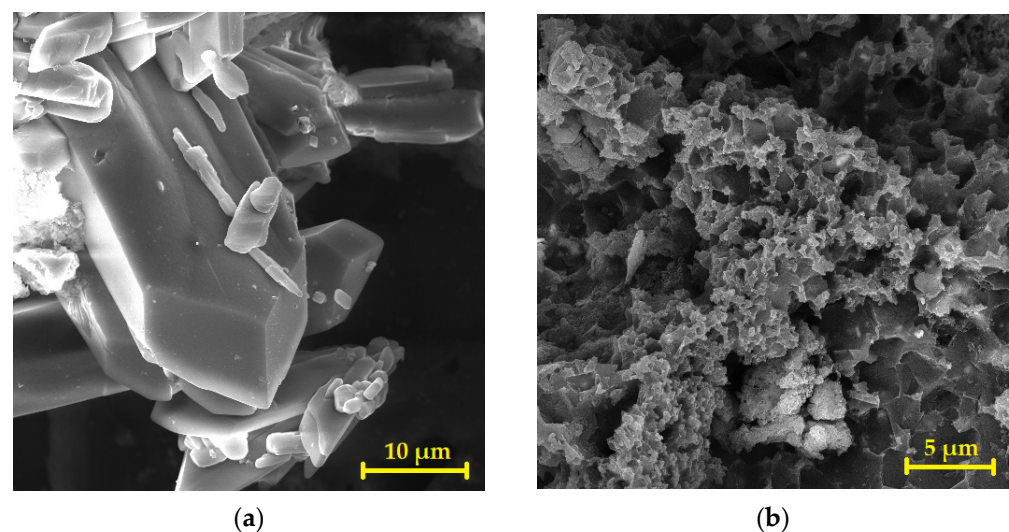


**Figure 15.** SEM photomicrographs of the coating after exposure to 30%  $\text{CH}_2\text{O}_2$  for 120 days: (a) NBR-CW containing shards exposed to the aggressive environment— $3000\times$  magnification; (b) NBR-REF with rounded particles— $5000\times$  magnification.

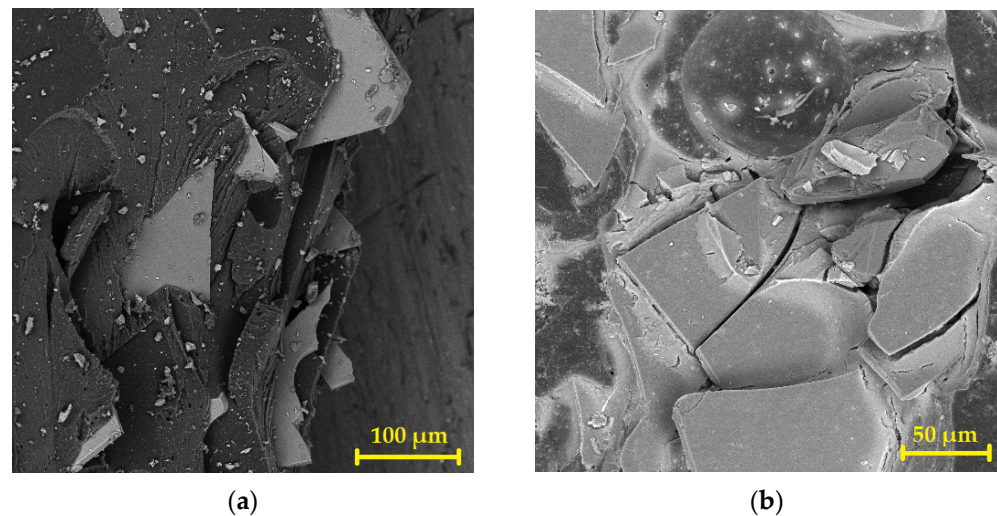


**Figure 16.** SEM photomicrographs of the coating NBR-GF containing glass flakes: (a) sample not exposed to the aggressive environment—300× magnification; (b) sample after exposure to 30%  $\text{CH}_2\text{O}_2$  for 90 days—500× magnification.

## 5. Conclusions

This research verified filler particle shapes' influence on the chemical resistance and chosen properties of epoxy coatings for concrete and monitored the basic properties of the epoxy-based polymer coatings. Individual coatings contained different types of waste glass as fillers or reference fillers for comparison of the monitored parameters. Furthermore, the content of glass flakes in the epoxy coating within the influence of the particle shape of the filler on chemical resistance was also monitored. Several findings are summarised as follows:

- The best properties, such as adhesion to concrete, hardness, tensile strength and chemical resistance, were reached by the NBR coating using 25% of windshield glass—shards as the filler (NBR-CW). The properties of this coating were similar to and, in several cases, even better than the properties of the reference coating on the same epoxy base containing silica flour.
- The shape of the filler grains significantly influenced how the whole polymer system degrades, i.e., there is degradation of the material in the form of peeling, or complete destruction of the material in the form of dust. On the other hand, the particle shape did not influence the level and rate of degradation of the polymer coating material.
- The loss of adhesion, gloss, colour and shape was observed as the first signal of the chemical degradation of the polymer during the experiment, while, according to theoretical findings, there was most likely defragmentation of the polymer chain (hundreds and thousands of atoms in the chain) to oligomers (dozens of atoms in the chain), and thus depolymerisation of the whole system of the tested material. Very slow depolymerisation—ageing of the polymer—can be positively used, for instance, for plastic recycling (biodegradation).
- The particle shape achieved while grinding the waste glass—shards—had no negative impact on the chemical resistance, but the polymer matrix filled with these shards reacted with the chemically aggressive environment in the same way and in the same time frame as a commercially produced material, either filled with glass flakes or silica flour.
- Polymer coatings containing waste glass of different origins are usable in the same way as commercially produced materials with the same or better properties.

**Author Contributions:** Conceptualisation, J.H. (Jana Hodná) and J.H. (Jakub Hodul); methodology, J.H. (Jana Hodná) and M.S.; validation, J.H. (Jakub Hodul), R.D. and M.S.; formal analysis, J.H. (Jana Hodná); investigation, J.H. (Jakub Hodul); resources, M.S. and R.D.; data curation, J.H. (Jana

Hodná) and J.H. (Jakub Hodul); writing—original draft preparation, J.H. (Jana Hodná) and J.H. (Jakub Hodul); writing—review and editing, J.H. (Jakub Hodul) and R.D.; project administration, R.D. and M.S.; funding acquisition, R.D. and M.S. All authors have read and agreed to the published version of the manuscript.

**Funding:** This research was funded by the Technology Agency of the Czech Republic, project ADMATEC—Advanced Materials and Technologies, subproject of TN01000056 CAMEB—‘Centre for Advanced Materials and Efficient Buildings’, Grant No. TN01000056/04.

**Institutional Review Board Statement:** Not applicable.

**Informed Consent Statement:** Not applicable.

**Data Availability Statement:** Data sharing is not applicable to this article.

**Conflicts of Interest:** The authors declare no conflict of interest.

## References

1. Faccini, M.; Bautista, L.; Soldi, L.; Escobar, A.M.; Altavilla, M.; Calvet, M.; Domènech, A.; Domínguez, E. Environmentally friendly anticorrosive polymeric coatings. *Appl. Sci.* **2021**, *11*, 3446. [\[CrossRef\]](#)
2. Sethi, J.; Afrin, S.; Karim, Z. Chapter seventeen—Smart polymer coatings for protection from corrosion. In *Smart Polymer Nanocomposites, Biomedical and Environmental Applications*; Bhawani, A.S., Khan, A., Jawaid, M., Eds.; Woodhead Publishing: Cambridge, UK, 2021; pp. 399–413.
3. Liu, J.; Yu, Q.; Yu, M.; Li, S.; Zhao, K.; Xue, B.; Zu, H.J. Silane modification of titanium dioxide-decorated graphene oxide nanocomposite for enhancing anticorrosion performance of epoxy coatings on AA-2024. *J. Alloys Compd.* **2018**, *744*, 728–739. [\[CrossRef\]](#)
4. Koblischek, P.J. Protection of surfaces of natural stone and concrete through polymers. In *Surface Engineering*; Meguid, S.A., Ed.; Springer: Dordrecht, The Netherlands, 1990; pp. 62–71.
5. Lokuge, W.; Aravinthan, T. Effect of fly ash on the behaviour of polymer concrete with different types of resin. *Mater. Des.* **2013**, *51*, 175–181. [\[CrossRef\]](#)
6. Zegardlo, B.; Szlag, M.; Ogrodnik, P.; Bombik, A. Physico-mechanical properties and microstructure of polymer concrete with recycled glass aggregate. *Materials* **2018**, *11*, 1213. [\[CrossRef\]](#)
7. Kim, W.; Soh, Y. Properties of unsaturated polyester mortars using crushed waste glass. *J. Asian Archit. Build. Eng.* **2018**, *1*, 7–12. [\[CrossRef\]](#)
8. Barcia, F.L.; Amaral, T.P.; Soares, B.G. Synthesis and properties of epoxy resin modified with epoxy-terminated liquid polybutadiene. *Polymer* **2003**, *44*, 5811–5819. [\[CrossRef\]](#)
9. Lorenzo, M.A. Experimental Methods for Evaluating Epoxy Coating Adhesion to Steel Reinforcement. Master’s Thesis, The University of Texas at Austin, Austin, TX, USA, 1997.
10. Norman, G.I. *Testing of Organic Coatings*; Noyes Data Corp.: Park Ridge, NJ, USA, 1977.
11. Zhang, Q.; Zhang, X.; Mu, X.; Wang, Z.; Tian, R.; Wang, X.; Liu, X. Recyclable waste image recognition based on deep learning. *Resour. Conserv. Recycl.* **2021**, *171*, 105636. [\[CrossRef\]](#)
12. Phakedi, D.; Ude, A.U.; Oladijo, P.O. Co-pyrolysis of polymer waste and carbon-based matter as an alternative for waste management in the developing world. *J. Anal. Appl. Pyrolysis.* **2021**, *155*, 105077. [\[CrossRef\]](#)
13. Rudolph, N.; Kiesel, R.; Aumnate, C. 7-Plastic waste around the world: Increasing potential of recycling. In *Understanding Plastics Recycling*, 2nd ed.; Carl Hanser: Munich, Germany, 2021; pp. 97–115.
14. Devi, S.V.; Gausikan, R.; Chithambarathan, S.; Jeffrey, J.W. Utilization of recycled aggregate of construction and demolition waste as a sustainable material. *Mater. Today Proc.* **2021**, *45*, 6649–6654. [\[CrossRef\]](#)
15. Zhou, A.; Zhang, W.; Wei, H.; Liu, T.; Zou, D.; Guo, H. A novel approach for recycling engineering sediment waste as sustainable supplementary cementitious materials. *Resour. Conserv. Recycl.* **2021**, *167*, 105435. [\[CrossRef\]](#)
16. Rani, M.; Choudhary, P.; Krishnan, V.; Zafar, S. A review on recycling and reuse methods for carbon fiber/glass fiber composites waste from wind turbine blades. *Compos. B Eng.* **2021**, *215*, 108768. [\[CrossRef\]](#)
17. Chowanec, A.; Sadowski, Ł.; Żak, A. The chemical and microstructural analysis of the adhesive properties of epoxy resin coatings modified using waste glass powder. *Appl. Surf. Sci.* **2020**, *504*, 144373. [\[CrossRef\]](#)
18. Saba, N.; Tahir, P.M.; Jawaid, M. A review on potentiality of nano filler/natural fiber filled polymer hybrid composites. *Polymers* **2014**, *6*, 2247–2273. [\[CrossRef\]](#)
19. Sørensen, P.A.; Kiil, S.; Dam-Johansen, K.; Weinell, C.E. Anticorrosive coatings: A review. *J. Coat. Technol. Res.* **2009**, *6*, 135–176. [\[CrossRef\]](#)
20. Abu-Thabit, N.Y.; Makhlof, A.S.H. Chapter 24—Recent advances in nanocomposite coatings for corrosion protection applications. In *Handbook of Nanoceramic and Nanocomposite Coatings and Materials*; Makhlof, A.S.H., Scharnweber, D., Eds.; Butterworth-Heinemann: Oxford, UK, 2015; pp. 515–549.

21. Zhang, X.; Xu, W.; Xia, X.; Zhang, Z.; Yu, R. Toughening of cycloaliphatic epoxy resin by nanosize silicon dioxide. *Mater. Lett.* **2006**, *60*, 3319–3323. [CrossRef]
22. Wetzel, B.; Hauptert, F.; Zhang, M.Q. Epoxy nanocomposites with high mechanical and tribological performance. *Compos. Sci. Technol.* **2003**, *63*, 2055–2067. [CrossRef]
23. Wang, G.; Yang, J. Influences of glass flakes on fire protection and water resistance of waterborne intumescent fire resistive coating for steel structure. *Prog. Org. Coat.* **2011**, *70*, 150–156. [CrossRef]
24. Ghaffari, M.; Ehsani, M.; Khonakdar, H.A. Morphology, rheological and protective properties of epoxy/nano-glassflake systems. *Prog. Org. Coat.* **2014**, *77*, 124–130. [CrossRef]
25. Nematollahi, M.; Heidarian, M.; Peikari, M.; Kassiriha, S.M.; Arianpouya, N.; Esmailpour, M. Comparison between the effect of nanoglass flake and montmorillonite organoclay on corrosion performance of epoxy coating. *Corros. Sci.* **2010**, *52*, 1809–1817. [CrossRef]
26. Pajarito, B.; Kobouchi, M. Flake-filled polymers for corrosion protection. *J. Chem. Eng. Japan* **2013**, *46*, 18–26. [CrossRef]
27. Wypych, G. 15—Fillers in commercial polymers. In *Handbook of Fillers*, 5th ed.; ChemTec Publishing: Toronto, ON, Canada, 2021; pp. 787–932.
28. Saravanan, P.; Jayamoorthy, K.; Kumar, S.A. Design and characterization of non-toxic nano-hybrid coatings for corrosion and fouling resistance. *J. Sci. Adv. Mater. Dev.* **2016**, *1*, 367–378. [CrossRef]
29. Hearn, R.C. Glassflake reinforced linings and coatings. *Anti-Corros. Methods Mater.* **1978**, *25*, 7–9. [CrossRef]
30. Pourhashem, S.; Saba, F.; Duan, J.; Rashidi, A.; Guan, F.; Nezhad, E.G.; Hou, B. Polymer/Inorganic nanocomposite coatings with superior corrosion protection performance: A review. *J. Ind. Eng. Chem.* **2020**, *88*, 29–57. [CrossRef]
31. Sathiyarayanan, S.; Azim, S.S.; Venkatachari, G. Corrosion protection coating containing polyaniline glass flake composite for steel. *Electrochim. Acta.* **2008**, *53*, 2087–2094. [CrossRef]
32. Solyndra: Its Technology and Why It Failed. Available online: <https://www.edn.com/solyndra-its-technology-and-why-it-failed/> (accessed on 25 January 2022).
33. ISO 4624:2016; Paints and Varnishes—Pull-Off Test for Adhesion. International Organization for Standardization (ISO) Technical Committee ISO/TC35/SC9: Geneva, Switzerland, 2016.
34. ISO 868:2003; Plastics and Ebonite—Determination of Indentation Hardness by Means of a Durometer (Shore Hardness). International Organization for Standardization (ISO) Technical Committee ISO/TC61/SC2: Geneva, Switzerland, 2003.
35. Liu, J.; Li, J.; Cheng, X.; Wang, H. Microstructures and tensile properties of laser clad AerMet100 steel coating on 300 M steel. *J. Mater. Sci. Technol.* **2018**, *34*, 643–652. [CrossRef]
36. ISO 527-1:2019; Plastics—Determination of Tensile Properties—Part 1: General Principles. International Organization for Standardization (ISO) Technical Committee ISO/TC61/SC2: Geneva, Switzerland, 2019.
37. ISO 527-2:2012; Plastics—Determination of Tensile Properties—Part 2: Test Conditions for Moulding and Extrusion, Plastics. International Organization for Standardization (ISO) Technical Committee ISO/TC61/SC2: Geneva, Switzerland, 2012.
38. Pedroza, G.A.G.; de Souza, C.A.C.; de Jesus, M.D.; de Andrade Lima, L.R.P.; Riberio, D.V. Influence of formic acid on the microstructure and corrosion resistance of Zn–Ni alloy coatings by electrodeposition. *Surf. Coat. Tech.* **2014**, *258*, 232–239. [CrossRef]
39. Ribeiro, M.C.S.; Tavares, C.M.L.; Ferreira, A.J.M. Chemical resistance of epoxy and polyester polymer concrete to acids and salts. *J. Polym. Eng.* **2002**, *22*, 27–44. [CrossRef]
40. Sharmin, E.; Imo, L.; Ashraf, S.M.; Ahmad, S. Acrylic-melamine modified DGEBA-epoxy coatings and their anticorrosive behavior. *Prog. Org. Coat.* **2004**, *50*, 47–54. [CrossRef]
41. Dellate, N.J.; Fowler, D.W.; McCullough, B.F.; Grater, S.F. Investigating performance of bonded concrete overlays. *J. Perform. Constr. Facil.* **1998**, *5*, 62–70. [CrossRef]
42. Manning, D.G. Corrosion performance of epoxy-coated reinforcing steel: North American experience. *Constr. Build. Mater.* **1996**, *10*, 349–365. [CrossRef]
43. Hodul, J.; Mészárosová, L.; Žlebek, T.; Drochytka, R.; Dufek, Z. Impact of aggressive media on the properties of polymeric coatings with solidification products as fillers. *Coatings* **2019**, *9*, 793. [CrossRef]
44. Momber, A.W.; Irmer, M.; Marquardt, T. Effects of polymer hardness on the abrasive wear resistance of thick organic offshore coatings. *Prog. Org. Coat.* **2020**, *146*, 105720. [CrossRef]
45. Hu, L.; Zhang, X.; Sun, Y.; Williams, R.J.J. Hardness and elastic modulus profiles of hybrid coatings. *J. Solgel. Sci Technol.* **2005**, *34*, 41–46. [CrossRef]
46. Declucchi, M.; Barbucci, A.; Cerisola, G. Crack-bridging ability and liquid water permeability of protective coatings for concrete. *Prog. Org. Coat.* **1998**, *33*, 76–82. [CrossRef]
47. Zheng, Y.; Zheng, Y.; Ning, R. Effects of nanoparticles SiO<sub>2</sub> on the performance of nanocomposites. *Mater. Lett.* **2003**, *57*, 2940–2944. [CrossRef]
48. Al-Turaif, H.A. Relationship between tensile properties and film formation kinetics of epoxy resin reinforced with nanofibrillated cellulose. *Prog. Org. Coat.* **2013**, *76*, 477–481. [CrossRef]
49. Almusallam, A.A.; Khan, F.M.; Dulaijan, S.U.; Al-Amoudi, O.S.B. Effectiveness of surface coatings in improving concrete durability. *Cem. Concr. Compos.* **2003**, *25*, 473–481. [CrossRef]

50. Dębska, B.; Lichołai, L. Long-term chemical resistance of ecological epoxy polymer composites. *J. Ecol. Eng.* **2018**, *19*, 204–212. [[CrossRef](#)]
51. González-Guzmán, J.; Santana, J.J.; Gonzáles, S.; Souto, R.M. Resistance of metallic substrates protected by an organic coating containing glass flakes. *Prog. Org. Coat.* **2010**, *68*, 240–243. [[CrossRef](#)]
52. Pacheco-Torgal, F.; Jalali, S. Sulphuric acid resistance of plain, polymer modified, and fly ash cement concretes. *Constr Build. Mater.* **2009**, *23*, 3485–3491. [[CrossRef](#)]
53. Tasnim, S.; Shaikh, F.U.A. Effect of chemical exposure on mechanical properties and microstructure of lightweight polymer composites containing solid waste fillers. *Constr. Build. Mater.* **2021**, *309*, 125192. [[CrossRef](#)]
54. Aggarwal, L.K.; Thapliyal, P.C.; Karade, S.R. Anticorrosive properties of the epoxy–cardanol resin based paints. *Prog. Org. Coat.* **2007**, *59*, 76–80. [[CrossRef](#)]